Boundary-Layer Meteorol (2014) 151:317–334
DOI 10.1007/s10546-013-9897-8

ARTICLE

Investigation of the Planetary Boundary Layer in the Swiss Alps Using Remote Sensing and In Situ Measurements

C. Ketterer · P. Zieger · N. Bukowiecki · M. Collaud Coen · O. Maier · D. Ruffieux · E. Weingartner

Received: 15 November 2012 / Accepted: 10 December 2013 / Published online: 10 January 2014

Abstract The development of the planetary boundary layer (PBL) has been studied in a complex terrain using various remote sensing and in situ techniques. The high-altitude research station at Jungfraujoch (3,580 m a.s.l.) in the Swiss Alps lies for most of the time in the free

C. Ketterer · P. Zieger (✉) · N. Bukowiecki · E. Weingartner
Laboratory of Atmospheric Chemistry, Paul Scherrer Institute, 5232 Villigen, Switzerland
e-mail: paul.zieger@itm.su.se

C. Ketterer
e-mail: Christine.Ketterer@meteo.uni-freiburg.de

N. Bukowiecki
e-mail: nicolas.bukowiecki@psi.ch

E. Weingartner
e-mail: ernest.weingartner@fhnw.ch

C. Ketterer · M. Collaud Coen · O. Maier · D. Ruffieux
Federal Office of Meteorology and Climatology, MeteoSwiss, Aerological Station, Ch. de l'Aérologie, 1530 Payerne, Switzerland
e-mail: Martine.Collaud@meteoswiss.ch

O. Maier
e-mail: olaf.maier@gmx.ch

D. Ruffieux
e-mail: dominique.ruffieux@meteoswiss.ch

Present Address
C. Ketterer
Meteorological Institute, Albert-Ludwigs-University Freiburg, 79085 Freiburg, Germany

Present Address
P. Zieger
Department of Applied Environmental Science, Stockholm University, 10691 Stockholm, Sweden

Present Address
E. Weingartner
Institute for Aerosol and Sensor Technology, University of Applied Science, Northwestern Switzerland, 5210 Windisch, Switzerland

troposphere except when it is influenced by the PBL reaching the station, especially during the summer season. A ceilometer and a wind profiler were installed at Kleine Scheidegg, a mountain pass close to Jungfraujoch, located at an altitude of 2,061 m a.s.l. Data from the ceilometer were analyzed using two different algorithms, while the signal-to-noise ratio of the wind profiler was studied to compare the retrieved PBL heights. The retrieved values from the ceilometer and wind profiler agreed well during daytime and cloud-free conditions. The results were additionally compared with the PBL height estimated by the numerical weather prediction model COSMO-2, which showed a clear underestimation of the PBL height for most of the cases but occasionally also a slight overestimation especially around noon, when the PBL showed its maximum extent. Air parcels were transported upwards by slope winds towards Jungfraujoch when the PBL was higher than 2,800 m a.s.l. during cloud-free cases. This was confirmed by the in situ aerosol measurements at Jungfraujoch with a significant increase in particle number concentration, particle light absorption and scattering coefficients when PBL-influenced air masses reached the station in the afternoon hours. The continuous aerosol in situ measurements at Jungfraujoch were clearly influenced by the local PBL development but also by long-range transport phenomena such as Saharan dust or pollution from the south.

Keywords Boundary layer · Ceilometer · Complex topography · In situ measurements · Jungfraujoch · Remote sensing · Switzerland · Wind profiler

1 Introduction

The planetary boundary layer (PBL) is the lowest part of the troposphere that is directly influenced by the Earth's surface—the layer next to the Earth's surface in which the effects of friction and surface heating are felt on a time scale of about 1 h or less (Stull 1988). While several PBL representations and studies have been designed for flat terrain (Garratt 1994; Wekker et al. 2004; Weigel 2005), knowledge of PBL behaviour over mountainous areas is rather incomplete to date. The few available studies are based on highly simplified and idealized parametrizations of mountains, undulating areas or valleys (Stull 1988; Whiteman 2000; Wekker et al. 2004; Weigel 2005). However, mountain ranges enable exchange processes, also called handover processes (Kossmann et al. 1998), i.e. mixing of PBL air masses into the free troposphere by cloud and mountain venting. Mountain venting describes the process by which upslope winds increase the altitude of the PBL height locally, and if strong enough, trigger the vertical exchange of PBL air into the free troposphere. Vice versa, air from the free troposphere can enter the PBL by entrainment, especially upwind of mountain ranges. Moreover, cloud venting defines the process between the PBL and free troposphere caused by cumulus formation in combination with strong upslope winds (Kossmann et al. 1999).

Based on these processes, the PBL—free troposphere dynamics are more complex in a region such as the Swiss Alps due to different thermal behaviour, mountain circulation, gap flows and other processes. However, there are examples that show very good agreement with a standard PBL description as e.g. described in Stull (1988) (Kossmann et al. 1998; Wekker et al. 2004; Weigel 2005). The typical diurnal cycle of the PBL is characterized by specific daytime and nighttime profiles of the virtual potential temperature, wind speed, water vapour mixing ratio and aerosol concentration. In situ or remote sensing measurement techniques are able to measure temperature, humidity, wind speed and aerosol backscattering profile that can be used to determine the PBL height. The bulk Richardson number and parcel

methods are commonly used to estimate the PBL height from temperature profiles (Stull 1988; Hennemuth and Lammert 2006).

An improved understanding of PBL development in complex terrain such as the Alps is particularly important to generally deepen our understanding and to improve the accuracy of numerical weather prediction. Furthermore, increased knowledge is needed to relate the local PBL influence to the long-term aerosol measurements performed continuously at Jungfraujoch. The comparison of the applied methods will also contribute towards a better understanding of the measurement techniques and methods used to characterize the PBL. The main research questions of this study can be formulated as follows:

1. How does the local complex topography influence the wind field?
2. Can slope and valley-mountain winds be unambiguously identified by remote sensing and in situ measurements?
3. Is the diurnal cycle of the high altitude PBL during convective days comparable to the PBL development over flat terrain?
4. How accurately can the PBL height be determined by the different remote-sensing instruments?
5. How do the measurements compare with predictions by the employed numerical weather prediction model?
6. How are the remote-sensing measured PBL heights and the in situ aerosol measurements at Jungfraujoch related?

2 Field Campaign

2.1 Site Description

The high-altitude research station at Jungfraujoch (JFJ, 46.5475°N, 7.9792°E) is situated in the Swiss Alps at 3,580 m a.s.l. and forms part of the Global Atmospheric Watch (GAW) program of the World Meteorological Organization (WMO). Jungfraujoch is a saddle between the mountain peaks Jungfrau (4,158 m a.s.l.) and Mönch (4,107 m a.s.l.) in the south-western and north-eastern directions. Kleine Scheidegg (KLS, 46.585°N, 7.9611° E, 2,061 m a.s.l.) is a mountain pass located approximately 4,800 m to the north-west of the JFJ station. Kleine Scheidegg is situated between Lauberhorn (2,472 m a.s.l.) and Eiger (3,970 m a.s.l.) and connects the two valleys, Grindelwald and Lauterbrunnen. In contrast to the JFJ station, the KLS site was a temporary field location equipped with instrumentation dedicated to this campaign. The Aletsch glacier, on the southern side of the JFJ, covers a large area with slightly decreasing terrain. Figure 1 depicts the topography of the alpine environment and the location of the two measurement sites.

The high elevation of the JFJ site allows for an investigation of the lower free troposphere during most of the year, except for spring and summer, when PBL air masses are transported upwards to the site. The mechanisms responsible for advecting the PBL air up to the JFJ station altitude are of convective and mechanical nature. Namely the PBL air is uplifted by the convective PBL growth process and mountain venting (Nyeki et al. 2000; Henne et al. 2005; Collaud Coen et al. 2011). Previous PBL studies at the JFJ site identified elevated aerosol layers that are transported by advection to the site (Nyeki et al. 2002). Lugauer et al. (1998) describe the transport of aerosols to the JFJ site that occurs most frequently under anticyclonic conditions. They divide the PBL into two regions; a PBL above the Swiss plateau (a region of lower altitude north of JFJ surrounded by the Alps to the south and by

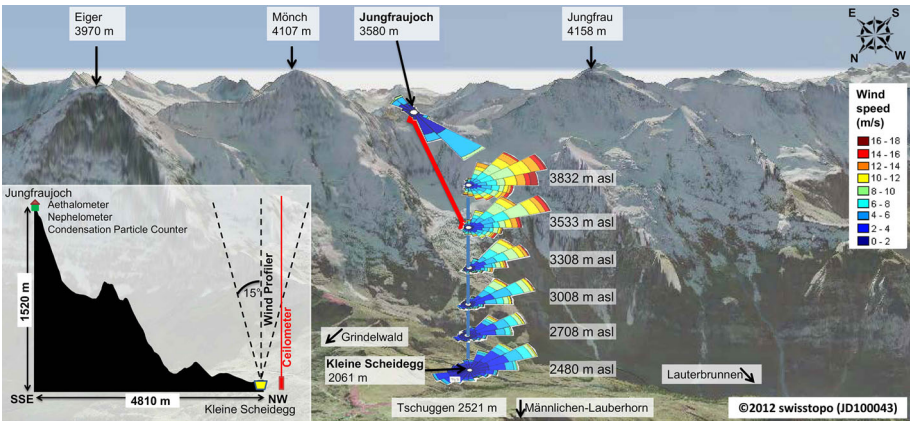

Fig. 1 Topographic image of the region Eiger, Mönch and Jungfrau in the Swiss Alps. The wind rose (wind direction and speed, see *colour code*) is shown using wind profiler high mode data at various altitudes above Kleine Scheidegg where also the ceilometer was installed. The in situ measurements of the wind speed and direction at Jungfraujoch were performed using a Rosemount anemometer, installed on top of a 10-m mast on the tourism platform (see Sect. 3.1)

the Jura mountains to the north-west) and a PBL above the Alps. The PBL air over the Swiss plateau can be transported by upslope winds to high-altitude sites. During transport PBL air is diluted by mixing with free tropospheric air (Collaud Coen et al. 2011). The uplifted PBL air parcels influence the vertical distribution of aerosols and trace gas from late spring to late summer and therefore affect the seasonal variability of aerosol properties at the JFJ site (see e.g. Baltensperger et al. 1997; Collaud Coen et al. 2011).

From June to August 2010, the Cloud and Aerosol Characterization Experiment (CLACE 2010) campaign took place at the JFJ and KLS sites (see Zieger et al. (2012) for an overview). During CLACE 2010, remote sensing instruments were installed at the KLS site including a wind profiler, a ceilometer, a sun photometer and a lidar. Zieger et al. (2012) discuss the vertical distribution of aerosol optical properties during this campaign.

2.2 Remote Sensing Instruments at Kleine Scheidegg

2.2.1 Wind Profiler

A wind profiler (LAP-3000, Vaisala Inc.) is a Doppler radar operating at $1{,}290 \times 10^6\ \mathrm{s}^{-1}$ with a wavelength of 23.3×10^{-2} m. Electromagnetic energy is emitted towards five beams with one vertical and four oblique beams tilted by 15° in the four orthogonal directions. The vertical resolution of the wind profiler was set to 74 m in the low mode and 204 m in the high mode. The minimum measurement height is about 340 m above ground and the maximum measurement height is 2,000–5,000 m above ground (depending on the atmospheric conditions).

The transmitted signal is partly scattered by refractive irregularities, which are caused by variations of air humidity, air temperature and air pressure at small scale. These refractive irregularities are advected with the wind and give information about the mean wind speed and direction. The obtained spectrum is characterized by its moments: a Doppler shift, a noise level, a signal power, a spectral width and a signal-to-noise ratio (SNR). The horizontal wind speed and direction are determined by combining the Doppler shifts of all beams for each range gate (Ecklund et al. 1988). The weak received signal is analyzed in the time-domain

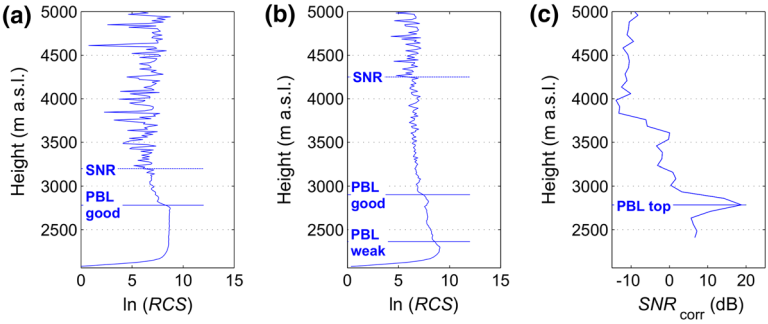

Fig. 2 Profiles of the logarithmic range-corrected signal (*RCS*) measured by the ceilometer on the 7 July 2010 at 1200 (**a**) and 2200 UTC (**b**). Indicated is the planetary boundary-layer height retrieved using the gradient method. Measured values below a signal-to-noise ratio of $SNR = 1$ (values above the *blue dashed line*) are disregarded. **c** Profile of the corrected signal-to-noise ratio SNR_{cor} retrieved from the wind profiler measurements and derived PBL height (*horizontal line*) recorded on the 7 July 2010 at 1200 UTC

and the frequency-domain steps (Ruffieux and Stübi 2001; Vaisala 2007). An important assumption is a homogeneous wind field over the beams' separation (Koscielny et al. 1984; Cheong et al. 2008), which cannot be fully guaranteed in the complex topography of the Alps.

The wind profiler measurement can additionally be used to retrieve an estimate of the PBL height. Small-scale turbulence causes variations of air temperature, air humidity and air pressure, which lead to variations in the refractive index of the air derived from the refractive structure parameter, which is proportional to the SNR of the wind profiler backscatter signal. Consequently, the range-corrected SNR can be an effective method of estimating the PBL height. The median of the SNR maximum of all four beams is considered as the PBL height (see the example in Fig. 2c). Herein, a method proposed by Angevine et al. (1994, 1998) is used. The distributed software from the manufacturer did not provide reasonable PBL heights and was therefore not further included in the analysis.

2.2.2 Ceilometer

A ceilometer (CHM15k, Jenoptik) measures the vertical profile of the aerosol backscatter at a wavelength of $\lambda = 1{,}064 \times 10^{-9}$ m, at a vertical resolution of 15 m and a pulse duration of 1×10^{-9} s (Jenoptik 2009). The signal due to the molecular scattering is almost negligible at $1{,}064 \times 10^{-9}$ m wavelength unless measured over a long integration time. The instrument is able to detect cloud layers and can also be used to estimate the PBL height. The signal is especially enhanced at the PBL top due to the hygroscopic growth of aerosols at high relative humidity.

Two different algorithms were used to analyze the PBL height from ceilometer recordings:

1. Gradient analysis: a multi-scale gradient analysis of ceilometer data is done using continuous Haar-wavelet transformation (Frey et al. 2010; Teschke and Poenitz 2010). The wavelet spectrum is derived, in which the maximum gradients are marked. Suitable layers are selected with the help of a *SNR* threshold ≥ 1, the value of the slope, and by comparing the values of the spatial and temporal neighbours.
2. STRAT-2D algorithm: the algorithm called "structure of the atmosphere" (STRAT-2D) uses a combination of wavelet covariance analysis and range-corrected signal (RCS)

Table 1 Quality index used for the planetary boundary-layer (PBL) height detection of the ceilometer measurement according to Haji and Wauben (2007)

Criteria	Classification	Colour used in the figures
$B_d - B_u < 0.25$	Poor PBL height detection	
$0.25 \leq B_d - B_u < 0.5$	Weak PBL height detection	
$B_d - B_u \geq 0.5$	Good PBL height detection	

The difference between the averaged logarithmic backscatter in the available range gates 150 m above (B_u) and below the boundary-layer height (B_d) is used at threshold

thresholding to estimate the PBL height from the measured range-corrected attenuated backscatter signal. Details of the algorithm can be found in Morille et al. (2007).

Figure 2a shows a RCS profile (logarithmic values) recorded on 7 July 2010 at 1200 UTC. The signal of the PBL is distinctive from 2,200 m a.s.l. to about 2,800 m a.s.l. The backscatter signal decreases with height above 2,250 m a.s.l. with two stronger gradients at 2,350 and 2,900 m a.s.l., which are marked as the top of the residual layers (Fig. 2b). To improve the results, the quality index of Haji and Wauben (2007) is applied to classify the PBL height estimations. For the calculation of the quality index, the backscatter is averaged in the available range gates 150 m above (B_u) and below the apparent PBL height (B_d). The calculated differences are divided into three classes that serve as a quality index (see Table 1).

2.3 In Situ Instrumentation at Jungfraujoch

Various aerosol in situ instruments are operated at the JFJ site on a continuous basis. A condensation particle counter (CPC; TSI Inc., Model 3772) measures the particle number concentration; an integrating nephelometer (TSI Inc., Model 3563) measures the particle light scattering coefficient at three wavelengths (450, 550 and 700×10^{-9} m), while an aethalometer (AE-31, Magee Scientific) is used to determine the aerosol absorption coefficient at seven different wavelengths. The aerosol in situ measurements are performed under dry conditions (relative humidity $<20\,\%$). In order to maintain dry conditions and to be able to use the inlet during harsh weather conditions, the aerosol instruments are connected to a heated inlet kept at about 25 °C. More information on the continuous in situ measurements can be found in Weingartner et al. (1999) and Collaud Coen et al. (2011); see also www.psi.ch/lac/jungfraujoch-site and https://gawrtl.psi.ch.

The wind speed and direction at the JFJ site were measured by a Rosemount pitot tube, mounted at the top of a 10-m mast and is part of the SwissMetNet network of MeteoSwiss.

2.4 The COSMO-2 Model

The COSMO-2 model (numerical weather prediction model consortium for small-scale modelling; see www.cosmo-model.org for more details) runs at a horizontal resolution of 2,200 m and with 60 vertical levels. It fully covers the region of Switzerland. The ECMWF global model (European Centre for Medium-Range Weather Forecasts, www.ecmwf.int) provides the boundary conditions for operational runs. COSMO-2 calculates the PBL height using the bulk Richardson number method (Szintai and Kaufmann 2007). The PBL heights at two grid

points closest to the KLS site were used in this study. The surface type of the first grid point is defined as "ice" (located at 7.963°N, 46.582°E, 1,956 m a.s.l.), while the second grid point is defined as "loam" (located at 7.962°N, 46.602°E and 1,753 m a.s.l.). The surface type of a grid point influences e.g. the temperature and humidity profiles due to the land-surface interactions. The temporal resolution used for this analysis is 1 h. The simulated PBL heights by COSMO-2 are defined as constant at 8 m above ground from sunset to sunrise.

3 Results

A fair-weather period with convective cloud formation, which often lead to precipitation and thunderstorms in the course of the day, dominated the first half of July 2010. Rainy and cooler weather with sunny intervals was predominant for the second half of July. Several fronts crossed the region in August 2010, causing cloudy and rainy weather and a declining snow line altitude (below 2,000 m a.s.l. at the end of August). The focus of this study was set on fair-weather days (7–9, 12, 20 and 31 July, as well as 7 and 9 August 2010).

3.1 Wind Profiler Versus In Situ Wind Measurements

Figure 1 shows the wind profiler and the in situ measurements of wind speed and direction for the entire CLACE 2010 campaign. With increasing altitude, the north-east component of the wind directions decreased while the south-west component and the wind speed generally increased due to reduced influence of the topography. Above approximately 3,500 m a.s.l. wind directions from the south-south-west to north were measured, although a south-west flow was prevailing. The influence of the Eiger, Mönch and Jungfrau mountains on the wind field is significant. South and south-east wind direction were rarely observed up to approximately 3,800 m, but the frequency of their occurrence increased above the altitude of the mountain peaks. The in situ wind measurement at the JFJ station showed mainly flow from the north-west and occasionally from the south-east. All other wind directions were negligible. The comparison between the in situ wind measurements at the JFJ site and the wind profiling at the KLS site shows that when a south-east wind direction was measured at the JFJ site, the wind profiler recorded flow from the south-west. Also, when the wind direction was from the north-west at the JFJ site, the wind profiler measured a west to north-west wind direction. This indicates that the wind directions are therefore first determined by the synoptic conditions but also largely influenced by the local topography, which shows a south-east to north-west orientation at the JFJ site and south-west to north-east orientation above the KLS site at the height of $2{,}480 \pm 102$ m.

3.2 Planetary Boundary-Layer Development in a High-Alpine Region

3.2.1 Case Study I: A Typical Mountainous PBL Development

Figure 3 shows a typical diurnal cycle of the PBL measured by the ceilometer (panel b) and the wind profiler (panel c). The COSMO-2 values are shown in addition to the results of the individual retrieval algorithms. For comparison, the schematic PBL development as e.g. described in Stull (1988) is shown in Fig. 3a.

Figure 3b shows the range-corrected backscatter signal (RCS) of the ceilometer and the PBL height calculated using both the gradient analysis and the STRAT-2D algorithm. Two declining residual layers from 4,200 to 3,200 m a.s.l. and from 3,450 to 2,500 m a.s.l. were

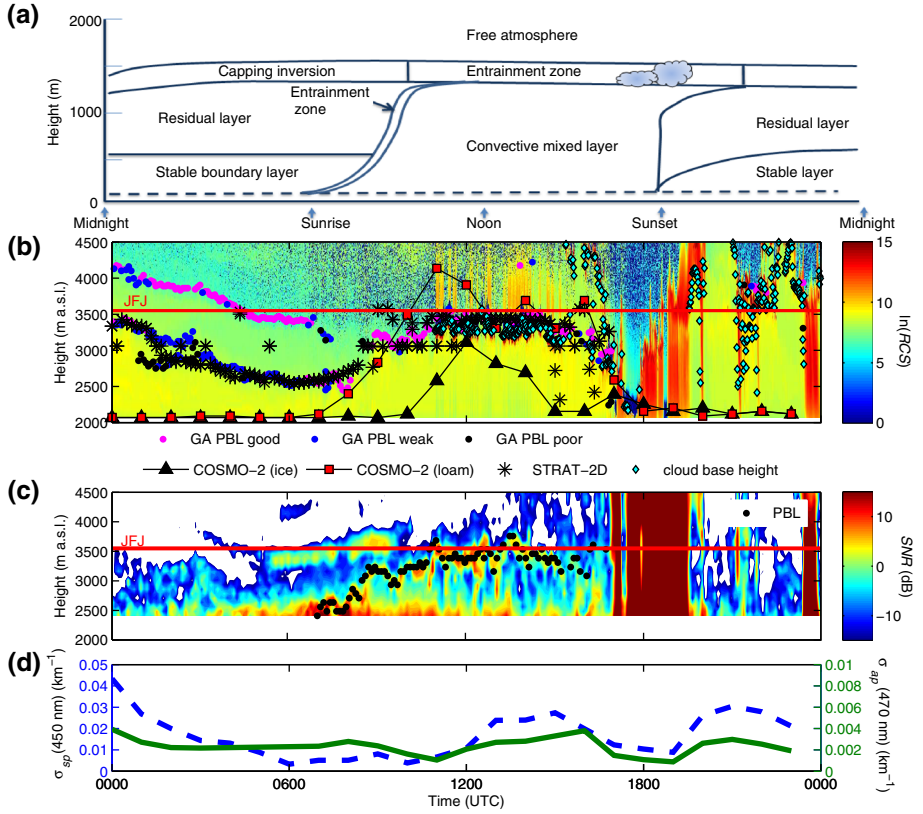

Fig. 3 **a** Typical diurnal PBL cycle, adapted from Stull (1988). **b** Range-corrected backscatter (*RCS*) of the ceilometer and planetary boundary-layer height determined using the gradient analysis (GA; *coloured points*) and STRAT-2D (*asterisks*) algorithm as well as cloud base height (*red dots*) for 12 July 2010. The boundary layer height predicted by the COSMO-2 model is shown for two grid points: ice (*black triangle*) and loam (*red square*). **c** *SNR* measured by the wind profiler and the retrieved planetary boundary-layer top (*black dots*). The *red line* in (**b**) and (**c**) depicts the height of the Jungfraujoch station. **d** Particle light scattering (*blue dashed line*) and absorption coefficients (*green solid line*) measured at the Jungfraujoch (hourly averages)

detected by both methods from midnight to 0700 UTC. The PBL increased after sunrise from 2,500 to around 3,500 m a.s.l., which was 1,500 m above ground and showed a plateau from 1300 to 1600 UTC (Fig. 3b). Convective clouds formed at the PBL top from 1100 to 1700 UTC, before precipitation set in, inhibiting further reliable detection of the PBL. Compared to the scheme of the typical diurnal PBL cycle (Fig. 3a) the convective boundary layer is similar, but two descending residual layers instead of one were observed above the KLS site (Fig. 3b) and can be interpreted as historic layers of the last few days.

The COSMO-2 derived PBL heights of grid point 1 (ice) and 2 (loam) increased sharply over daytime to 3,150 and 4,100 m a.s.l., respectively. In the afternoon, the PBL height fell below 2,500 m a.s.l., while the PBL height of the second point varied around 3,500 m and declined below 2,200 m. COSMO-2 does not consider residual layers. As mentioned above, the differences of the PBL heights between these two grid points are caused by the different surface types and subsequently different heating rates, temperature and humidity profiles of the atmosphere above. The differences between the two retrievals during the afternoon could

be caused by different cloud cover or the onset of simulated rain within the model. However, both PBL heights declined to around 2,200 m a.s.l. at 1700 UTC as a result of the modified potential temperature profile after sunset. The bulk Richardson number method, which was used by COSMO-2, detected the stable boundary layer during the night, which is not the same layer as detected by the remote sensing instruments and therefore not comparable.

Figure 3c depicts the range-corrected SNR of the wind profiler and the derived PBL height. The development of the PBL during daytime is almost identical to that observed by the wind profiler compared to the ceilometer measurements. However, the wind profiler fails to detect the different layers during nighttime because of a too-low SNR due to the stable atmosphere and the large instrumental overlap for the lowest layer. The PBL height also increased from 2,450 to 3,500 m and remained between 3,100 and 3,500 m a.s.l. until precipitation set in. During periods with clouds in the afternoon, the maximum SNR was found at the cloud top, which is not necessarily the PBL top. The ceilometer detects, on the other hand, the largest aerosol gradient at the height of the cloud-base. However, the determination of the PBL height becomes ambiguous in cloudy conditions as its definition remains itself ambiguous under these conditions.

The dry aerosol scattering and absorption coefficients measured at the JFJ site (hourly average, see Fig. 3d) decreased from midnight to 0600 UTC, corresponding to the decreasing residual layers. Both parameters increased after 1000 UTC until precipitation started at around 1700 UTC. During precipitation the aerosols were scavenged by the rain leading to a temporal minimum of both parameters between 1700 and 1900 UTC. After the cessation of rain, both parameters increased again to their previous values as the advected air was not affected by precipitation and the wash-out of particles.

3.2.2 Case Study II: Influence of the Local Wind Field

Wind profiler measurements of wind speed and direction are shown in addition to the different derived PBL heights in Fig. 4. The alpine PBL is strongly influenced by the local wind field. The wind profile could be divided into three decoupled regimes characterized by different wind direction and speed values: a gradient wind from the north above 3,450 m, a south-west thermal wind below 3,450 m and a wind regime within the PBL. A pronounced wind regime was established within the PBL, which is characterized by low horizontal wind speed and strong daytime updrafts. Strong updrafts also appeared in the early morning from 0630 to 0830 UTC at around 2,600 to 3,200 m height. These updrafts might be caused by a standing lee wave, which was produced by strong northerly winds crossing the Lauberhorn-Männlichen mountain range (located to the west of the KLS site in a south-north direction, see Fig. 1).

Figure 4 shows two declining layers; one from 3,600 to 2,800 m and another from 2,800 to 2,300 m a.s.l. that were observed above the KLS site from midnight until sunrise, similar to the first case (Fig. 3). After sunrise, the PBL height grew rapidly after 0600 UTC to reach a maximum of 3,000 m a.s.l. at around 1400 UTC. The maximum height of the PBL was about 3,000 m a.s.l. as measured by both instruments. In the daytime, the aerosol gradient at the top of the PBL was enhanced and a clear PBL signal was detected by both the wind profiler and the ceilometer. Whereas in the nighttime, the gradient was less pronounced and the quality of the detected residual layers was weak. Clouds formed at the top of the PBL (red crosses in Fig. 4) from 1400 to 1700 UTC as the thermals reached the lifting condensation level. Radiative cooling due to clouds induces sinking air parcels from the cloud top towards the Earth's surface (negative vertical wind velocity).

Two decreasing layers, one after the other, were observed in the transition zone in the late afternoon. The occurrence of these residual layers can be explained by the influence of the

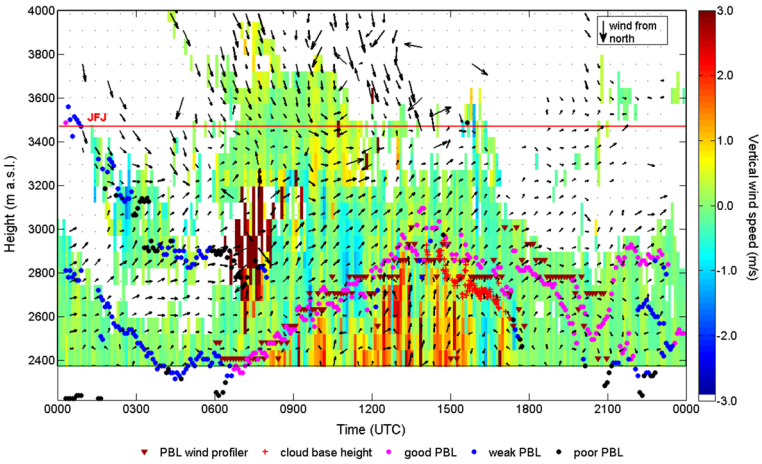

Fig. 4 Vertical wind speed (see *colour bar*, *negative values* are downdraft and *positive values* updraft winds), horizontal wind speed (length of *arrows*) and wind direction (orientation of *arrows*) measured by the wind profiler on 7 July 2010. PBL heights determined by the ceilometer and coloured according to the quality indices (*dots*, *colour* see Table 1), and by the wind profiler (*dark red triangles*). The cloud-base height measured by the ceilometer is shown as *red crosses*

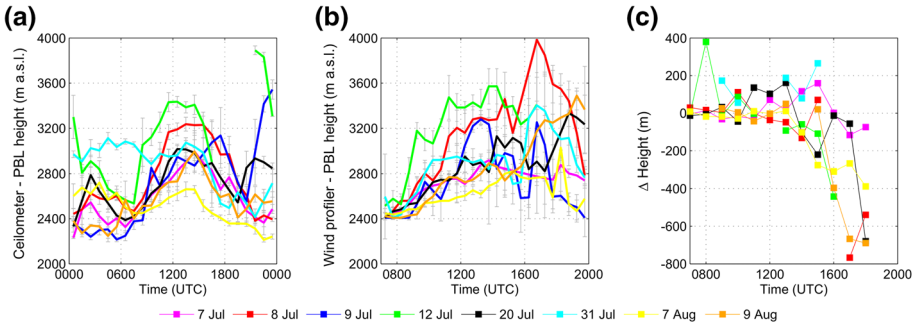

Fig. 5 Diurnal series of PBL heights measured by the ceilometer (**a**) and wind profiler (**b**). *Grey error bars* denote the standard deviation of each hour. **c** Depicts the differences (ceilometer—wind profiler) of the retrieved PBL heights for here shown fair weather days (see legend below)

local wind, changing clockwise from south to north successively in time with very low wind speeds. The development of these descending layers in the afternoon is not straightforwardly explained (e.g. by Stull (1988) and Garratt (1994)) and little is known about the decay of the PBL to date (Pino 2011). However, the descending layers were observed by both the wind profiler and the ceilometer.

3.2.3 Comparison of PBL Heights on Different Fair Weather Days

Figures 5a, b show all diurnal courses of the PBL height retrieved from the ceilometer (gradient analysis algorithm) and the wind profiler (hourly averages). The PBL heights determined by the ceilometer showed mainly decreasing heights of the aerosol layer at night an increase after sunrise with a peak during 1200 to 1400 UTC and a decreasing PBL in the afternoon hours. The maximum height of the PBL above the KLS site was 3,500 m a.s.l. and

the average minimum-to-maximum increase was about 500 m during fair weather days. Several exceptions are caused by long-range transported Saharan dust (see Zieger et al. 2012). Saharan dust might lead to a wrong estimate of the PBL height, e.g. in the evening of the 9 July, and an increasing PBL height was observed by the ceilometer, which rather displayed the upper boundary of the large Saharan dust plume. The PBL height detected in the evening of the 12 July marked rather the aerosol gradient above the clouds after precipitation than the real PBL top.

The highest and lowest PBL heights were detected by the wind profiler on 12 July (3,600 m) and on 7 August (2,800 m), respectively (Fig. 5b). As mentioned above, the wind profiler can only accurately retrieve PBL heights in the daytime. The wind profiler-retrieved PBL height grew on average by 130 m h^{-1} from 0700 to 1300 UTC and then peaked on average at 1400 UTC and remained almost constant in the afternoon. In the evening, when the PBL height decreased, a second descending layer of maximum SNR was measured; this declining layer was 300–550 m higher than the first. The highest layer had a greater SNR, which was primarily detected by the wind profiler (e.g. on 8 July 2010 a distinct second aerosol layer was seen). This second descending layer might be due to the pronounced wind shear in the evening.

Generally, a period of predominant convective anticyclonic synoptic weather, characterised by low horizontal and relatively high vertical wind speeds, lead to increased PBL heights during 7–12 July, as observed by both methods (see Fig. 5). This behaviour corresponds to the results of Lugauer et al. (1998).

3.3 Comparison of Different Methods for PBL Estimation

3.3.1 Performance of the Ceilometer Algorithms

Two different algorithms, STRAT-2D and the gradient analysis, were compared during fair weather conditions. Comparisons were made for both the entire day and daytime measurements. In general, the STRAT-2D algorithm retrieved higher PBL heights than the gradient analysis method (see Fig. 6a) and it indicated an offset of -210 ± 72 m over daytime and -120 ± 46 m over the entire day. The squared correlation coefficient R^2 of 0.79 was calculated in the daytime and 0.70 for the entire day. The uncertainty of the best fit coefficients

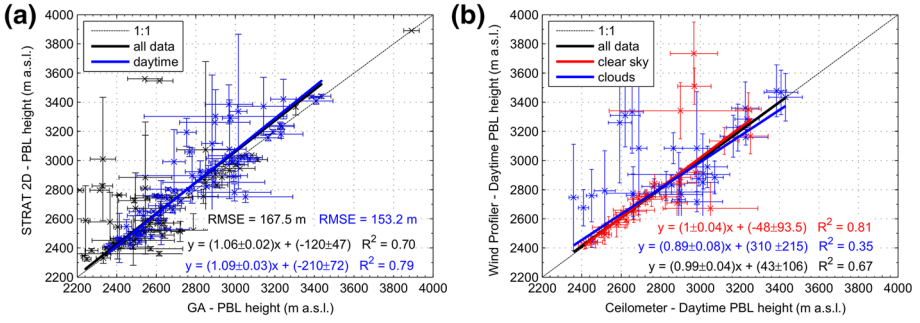

Fig. 6 **a** Comparison of PBL heights derived by the STRAT-2D and the gradient analysis algorithms on the defined fair weather days (*black points*) and only for daytime (*blue points*). **b** PBL height retrieved the from wind profiler versus the ceilometer (GA-algorithm) retrieved values. *Red points* are clear-sky cases, while *blue points* are cloud influenced. Only ceilometer values classified as good or weak are shown. The bivariate weighted fit with the given uncertainty (*solid lines*) is described in York et al. (2004). Hourly averaged values are shown in both panels

given in Fig. 6 was calculated according to the method in York et al. (2004). The root-mean-square error $RMSE = 153$ m was found in daytime and 168 m over the whole day. The difference between the nighttime and the daytime measurements was probably caused by the residual layers that were not always similarly detected by both algorithms. Moreover, the differences can be related to the depth of the capping inversion as well as to the uncertainties of both algorithms. However, the agreement between the two algorithms can be regarded as good. The results from the gradient analysis could be improved by the use of the quality method as described in Haji and Wauben (2007), which significantly reduces the number of outliers. In contrast, the STRAT-2D algorithm already includes a quality control of the layer determination and attribution to reduce the number of outliers.

3.3.2 Ceilometer Versus Wind Profiler PBL Determination

The derived PBL heights from the ceilometer (gradient analysis) and the wind profiler agreed well during daytime, especially on clear sky days (Fig. 6b). The slope of the orthogonal linear regression is 0.99 for the entire period, an offset value of 43 ± 106 m and $R^2 = 0.67$. During clear sky conditions, the correlation between both instruments is larger ($R^2 = 0.8$), whereas during cloudy conditions the correlation is weaker ($R^2 = 0.35$) with a smaller slope (0.89) and a large offset (310 ± 215 m). The correlation between PBL heights calculated using STRAT-2D and that derived from the wind profiler is weak, too, with an $R^2 = 0.47$ and a slightly greater *RMSE* (258 m compared to 233 m). The generally higher PBL tops derived from the wind profiler can be explained by the fact that the wind profiler often measured the higher of the two decreasing layers in the afternoon, whereas the PBL height detected by the ceilometer was always lower. This can also be seen in Fig. 5c, which depicts the hourly differences between the PBL derived by the ceilometer and the wind profiler. Until 1500 UTC, the difference between both instruments is mainly within ± 100 m, but in the late afternoon the differences become larger. Both instruments did not precisely perform during periods with clouds. The strongest aerosol gradient measured by the ceilometer was somewhere within the cloud, which might not be the top of the PBL (Wang et al. 2012). Cloud tops can occur below the PBL top, in the entrainment zone, or above the PBL (Stull 1988). The refractive index has also a maximum above the clouds due to the large gradient of humidity and turbulence, as well as the occurrence of wind shear (Grimsdell and Angevine 1998; Bianco and Wilczak 2002).

On the contrary, "considerable differences between PBL and aerosol layer" were observed in the Swiss Alps (Wekker et al. 2004). The literature describes the convective boundary layer as a PBL that follows the terrain (Wekker et al. 2004) or as a layer that is decoupled from the terrain (Kossmann et al. 1998). On the other hand, an aerosol layer is nearly uniform in height and generally does not follow the underlying terrain on a scale up to tens of km (Nyeki et al. 2000; Wekker 2002). The difference between the aerosol layer and PBL follows a daily cycle, and at night the aerosol or residual layer is deeper than the stable boundary layer. Therefore, the convective boundary-layer height follows the terrain during the morning, while the aerosol layer can be 1–2 km deeper than the PBL in a valley. As the convective boundary layer grows rapidly after sunrise, the difference between the convective PBL and the aerosol layer height becomes smaller.

3.4 PBL Measurements Compared with COSMO-2

The PBL height at the two grid points of the COSMO-2 model closest to the KLS site, which are also chosen based on similarity criteria of the surface type with the KLS site, were

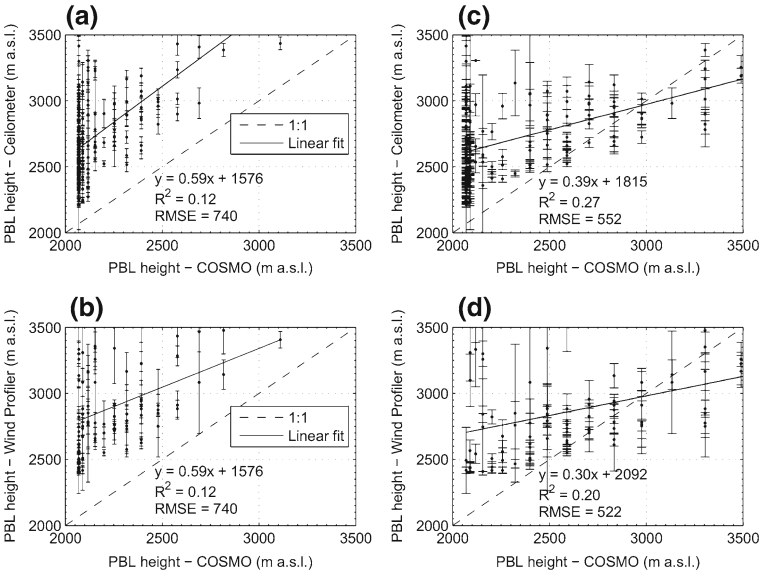

Fig. 7 PBL heights measured by the ceilometer (*upper panels*) and the wind profiler (*lower panels*) versus the calculated values of the COSMO-2 model for fair weather days at daytime. The *left panels* show the grid point defined as "ice", while the *right panels* show the value of the grid point defined as "loam". Both grid cells are within a distance of ≈3 km closest to Kleine Scheidegg. The *solid black line* represents a linear least squares regression. The squared correlation coefficient and the root-mean-square error (*RMSE*) are given as well

analyzed. The simulated PBL height is compared with the PBL height determined by the ceilometer (gradient analysis algorithm) and the wind profiler (Fig. 7). The PBL height of the first point (ice) shows a clear negative offset of 392 m compared to the PBL height derived from the ceilometer, and a slightly biased negative offset compared to the wind profiler. The comparison with the second point (loam) shows strong biased offsets of 1,815 m (ceilometer) and 2,092 m (wind profiler). The correlations are weak (R^2 between 0.12 and 0.27) and the *RMSE* is large (522 and 740 m). The observed weak correlations are perhaps due to the bulk Richardson number method used in the COSMO-2 model, which is based on the virtual potential temperature profiles, hence a different physical parameter than that used for ceilometer and wind profiler methods. Possible reasons for the disagreement can be the grid resolution and parametrization schemes, and the surface did not match the real topography. Additionally, there are uncertainties in the meteorological profiles or uncertainties within the bulk Richardson number method in general. Furthermore, the comparison between a single measurement point and a grid point is limited. There is also a challenge of developing a correct simulation of this complex environment and topography within the model.

3.5 Influence of PBL on In Situ Measurements at Jungfraujoch

The diurnal cycles of the particle light absorption coefficient σ_{ap} ($\lambda = 470 \times 10^{-9}$ m), particle light scattering coefficient σ_{sp} ($\lambda = 450 \times 10^{-9}$ m) and particle number concentration N are shown in Fig. 8a–c. The particle light absorption coefficient is characteristic of polluted air masses. The absorption and scattering coefficients had a similar diurnal cycle with a minimum at 0500 UTC and a maximum in the afternoon at around 1600 UTC. The absorption

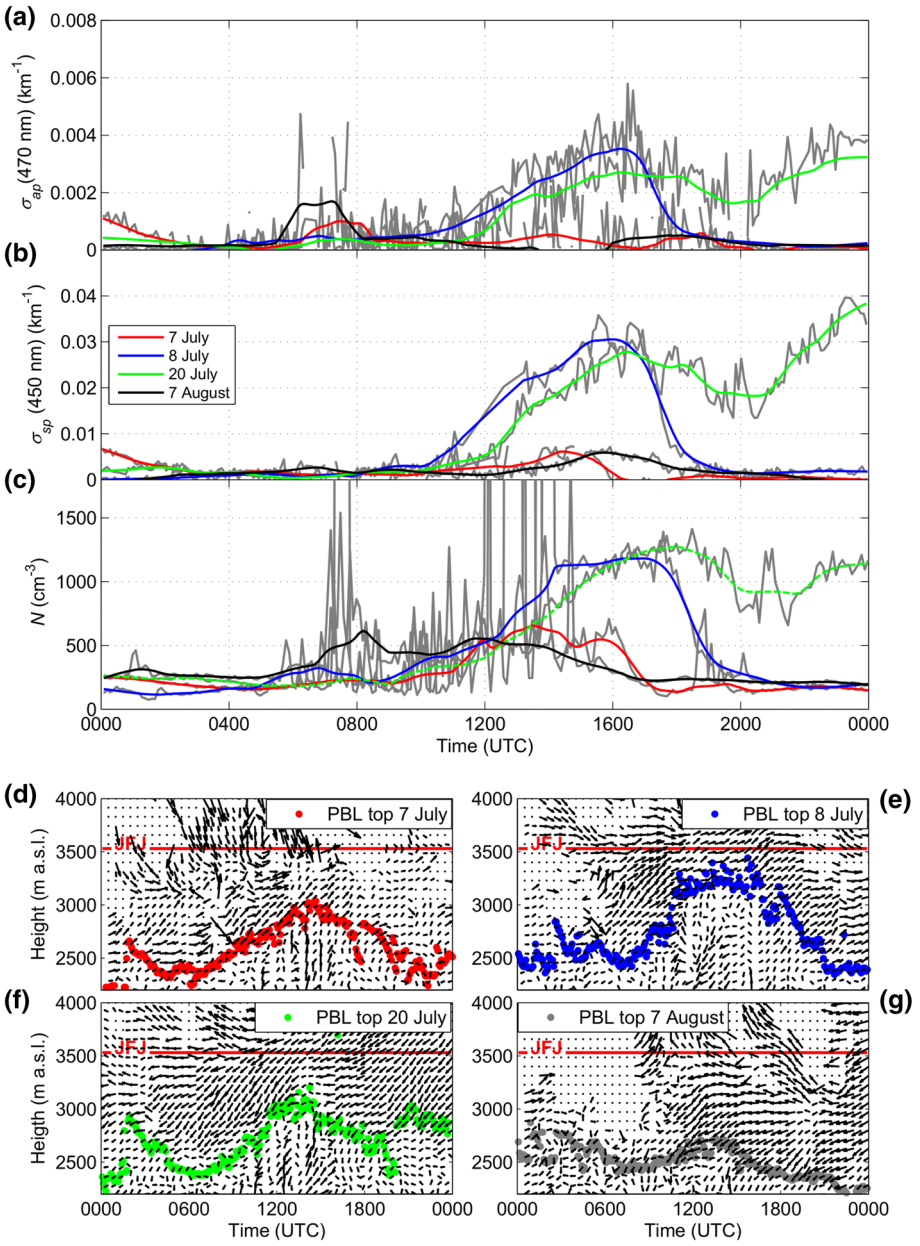

Fig. 8 Time series of the particle light absorption coefficient (**a**), particle light scattering coefficient (**b**), and particle number concentration (**c**). The *coloured lines* depict a moving average over 2 h, while the *grey lines* denote the raw data for selected days (see legend). **d–g** show the corresponding wind directions and wind speeds measured by the wind profiler and the corresponding PBL height derived from the ceilometer (gradient analysis retrieval)

and scattering coefficients usually decreased during evening and night (Collaud Coen et al. 2011), but in these cases they stayed on a high level during the afternoon and evening until 2300 UTC and decreased when the air mass was replaced by free tropospheric air.

Particle number concentration is a measure for both aged particles and for new Aitken-mode particles that are freshly formed from gaseous precursors (Weingartner et al. 1999). The daily cycle of N had a minimum at 0600 UTC and peaked at 1400 UTC. The distinct spikes of σ_{ap} ($\lambda = 470 \times 10^{-9}$ m) and N between 0700 and 1000 UTC were caused by local pollution events due to the use of a snowcat and other tourist activities at the JFJ station. Particle number concentration decreased in the afternoon and stayed at low level in the nighttime, when free tropospheric air replaced the air at the JFJ site, except for periods where the PBL air arrived at the JFJ site on 8, 9, 12 and 20 July 2010 in the afternoon.

During fair weather days, a clean relation between PBL height and the in situ measurements existed. On the 8 July 2010, the PBL showed a maximum at 3,250 m a.s.l. above the KLS site at 1300 UTC (Fig. 8e). Absorption and scattering coefficients (Fig. 8a, b) greatly increased from 1200 UTC showing a maximum at 1600 UTC. After 1800 UTC both coefficients decreased rapidly towards the usual low nocturnal level. The air parcels of the PBL were measured at the JFJ site, although the measured PBL height above the KLS site was 300 m lower than the JFJ altitude. The transport of PBL air upwards can be explained by strong upslope winds, which were observed by the wind profiler (see example of 7 July in Fig. 4). Therefore, the absolute height of the PBL was higher at the JFJ site than at the KLS site, while the PBL height above ground remained much lower at the JFJ site than at the KLS station. On 9 July 2010, the diurnal PBL increased only to about 3,200 m a.s.l. (Fig. 5); in the evening an aerosol layer comprising long-range transported Saharan dust was detected and observed by all in situ aerosol measurements. Scattering and absorption coefficients did not decrease as much as on 7 July, but remained high until midnight. The aerosol layer detected by the ceilometer in the late evening might be a gradient caused by a layer of Saharan dust. On 20 July 2010 (Fig. 8f), the scattering and the absorption coefficients remained high in the evening when also the residual layer showed little variations compared to the noon height (see Fig. 3a). The wind direction at the JFJ site changed in the late afternoon from north to south. This south wind transported polluted air from the Rhone valley across the glacier to the JFJ site. On the contrary, the PBL stayed below 3,000 m a.s.l. on the 7 and 31 July as well as on the 7 and 9 August (see Figs. 8d, g; 5), so that no high increase in absorption and scattering coefficients was detected at JFJ (Fig. 8a, b, cases of 9 and 31 July as well as 9 August are not being shown). The measured increase in particle number concentration during daytime is due to new particle formation and subsequent growth, since it is the only aerosol parameter presented in this study that is sensitive to the very small Aitken mode particles.

We found a good agreement between the remote-sensing and in situ measurements. Due to topography and transport by upslope winds, the PBL air is measured at the JFJ if the PBL height, detected by remote sensing instruments, is at least 2,800 m above the KLS site.

4 Conclusions

The wind direction greatly depends on the local topography and a comparison of the measurements at both mountain sites is difficult to be done in most cases. In situ and remote wind measurements should therefore be compared with great care. During fair weather days the PBL above JFJ follows a standard diurnal cycle with residual and convective layers during night and day, respectively. Besides the standard behaviour, the PBL also shows more complex structures, such as two subsiding aerosol layers during the afternoon and two declining residual layers, interpreted as “historic layers”. These two findings were unexpected and are not found in the common literature. A good agreement was found between the boundary-layer height determined by the ceilometer and the wind profiler during daytime, especially

for periods without clouds. Consequently, we conclude that the aerosol layer top measured by the ceilometer seemed to be consistent with the convective boundary-layer top, which is detected by the wind profiler. A full diurnal cycle of the boundary-layer height variations could only be detected using a ceilometer. The agreement between the calculated boundary-layer height of the numerical weather prediction model COSMO-2 and the measurements was found to be poor, with low correlation coefficient and large offsets. Possible reasons are the not optimal resolution of implemented topography within the model, the model retrieval method, and the quality of the input data. In addition, one has to keep in mind that a point measurement is compared to a PBL height of the entire grid cell. However, further improvement of numerical models for complex terrains like the Alps is highly desirable to provide an accurate weather prediction. The in situ aerosol measurements at Jungfraujoch were strongly influenced by the planetary boundary-layer development above Kleine Scheidegg. The PBL top at Jungfraujoch showed a clear similarity to the boundary-layer height measured above Kleine Scheidegg, if the effect of upslope winds were taken into account. Thereby, it could be concluded that the boundary-layer air is observed within a time delay of a few hours at Jungfraujoch, although the boundary-layer height above Kleine Scheidegg is some hundreds of metres lower than the altitude of Jungfraujoch. This air mass persisted at Jungfraujoch station until replaced by free tropospheric air in the late evening. Besides a boundary-layer influence, particle light absorption and scattering coefficients were influenced by long range transport of Saharan dust, precursor gas concentrations and photochemical processes in the free troposphere causing secondary aerosol formation. Furthermore, advection of aerosol and transport of pollutions from the south to Jungfraujoch influenced the measurements and hampered the correlation between the in situ and remote sensing measurements.

Acknowledgments We thank the International Foundation High Altitude Research Stations Jungfraujoch and Gornergrat (HFSJG) for providing the excellent infrastructure at Jungfraujoch. We also acknowledge the Jungfraubahnen for providing the infrastructure at Kleine Scheidegg. We thank Steffen Frey, Holger Wille and Kornelia Poenitz (Jenoptics) for their support and for lending the ceilometer. Pirmin Kaufmann and André Walser are acknowledged for providing the COSMO-2 data. This work was supported by MeteoSwiss within the Global Atmosphere Watch program (GAW) of the World Meteorological Organization (WMO). Thanks go to Yohann Morille and Martial Haeffelin for providing the STRAT-2D algorithm. Giovanni Martucci and Emmanuel Ndetto are acknowledged for reading the manuscript.

References

Angevine W, White A, Avery S (1994) Boundary-layer depth and entrainment zone characterization with a boundary-layer profiler. Boundary-Layer Meteorol 68:375–385

Angevine W, Bakwin P, Davis K (1998) Wind profiler and RASS measurements compared with measurements from a 450-m-tall tower. J Atmos Ocean Technol 15:818–825

Baltensperger U, Gäggeler H, Jost D, Lugauer M, Schwikowski M, Weingartner E, Seibert P (1997) Aerosol climatology at the high-alpine site Jungfraujoch, Switzerland. J Geophys Res 102:19707–19715

Bianco L, Wilczak J (2002) Convective boundary layer depth: improved measurement by Doppler radar wind profiler using fuzzy logic methods. J Atmos Ocean Technol 19:1745–1758

Cheong B, Palmer R, Yu T, Yang K, Hoffman M, Frasier S, Lopez-Dekker F (2008) Effects of wind field inhomogeneities on Doppler beam swinging revealed by an imaging radar. J Atmos Ocean Technol 25: 1414–1422

Collaud Coen M, Weingartner E, Furger M, Nyeki S, Prévôt A, Steinbacher M, Baltensperger U (2011) Planetary boundary influence at the Jungfraujoch analyzed by aerosol cycles and synoptic weather types. Atmos Chem Phys 11:10011–10030

de Wekker S (2002) Structure and morphology of the convective boundary layer in mountainous terrain. Dissertation, The University of British Columbia, 191 pp
de Wekker S, Steyn D, Nyeki S (2004) A comparison of aerosol-layer and convective boundary-layer structure over a mountain range during Staaarte '97. Boundary-Layer Meteorol 113:249–271
Ecklund W, Carter D, Balsley B (1988) A UHF wind profiler for the boundary layer: brief description and initial results. J Atmos Ocean Technol 5:432–441
Frey S, Poenitz K, Teschke G, Wille H (2010) Detection of aerosol layers with ceilometers and the recognition of the mixed layer depth. In: Proceedings of international symposium for the advancement of boundary layer remote sensing, Paris, 28–30 June 2010, 4 pp
Garratt JR (1994) The atmospheric boundary layer, 1st edn. Cambridge, University Press, Cambridge, 316 pp
Grimsdell A, Angevine W (1998) Convective boundary layer height measurement with wind profilers and comparison to cloud base. J Atmos Ocean Technol 15:1331–1338
Haji M, Wauben W (2007) Continuous mixing layer height determination using the LD-40 ceilometer: a feasibility study. De Bilt, Utrecht, 98 pp
Henne S, Dommen J, Neininger B, Reimann S, Staehelin J, Prévôt A (2005) Influence of mountain venting in the Alps on the ozone chemistry of the lower free troposphere and the European pollution export. J Geophys Res 110(D22307):1–18
Hennemuth B, Lammert A (2006) Determination of the atmospheric boundary layer height from radiosonde and lidar backscatter. Boundary-Layer Meteorol 120:181–200
Jenoptik (2009) CHM15k/CHM15-kx Wolkenhöhenmessgerät (Ceilometer). Bedienerhandbuch, Jena, 73 pp
Koscielny A, Doviak R, Zrnic D (1984) An evaluation of the accuracy of some radar wind profiling techniques. J Atmos Ocean Technol 1:309–320
Kossmann M, Vögtlin R, Corsmeier U, Vogel B, Fiedler F, Binder H, Kalthoff N, Beyrich F (1998) Aspects of the convective boundary layer structure over complex terrain. Atmos Environ 32:1323–1348
Kossmann M, Corsmeier U, de Wekker S, Fiedler F, Vögtlin R, Kalthoff N, Güsten H, Neininger B (1999) Observations of handover processes between the atmospheric boundary layer and the free troposphere over mountainous terrain. Contrib Atmos Phys 72:329–350
Lugauer M, Baltensperger U, Furger M, Gäggeler H, Jost D, Schwikowski M, Wanner H (1998) Aerosol transport to the high Alpine sites Jungfraujoch (3454 m a.s.l.) and Colle Gnifetti (4452 m a.s.l.). Tellus B 50:76–92
Morille Y, Haeffelin M, Drobinski P, Pelon J (2007) STRAT: an automated algorithm to retrieve the vertical structure of the atmosphere from single-channel lidar data. J Atmos Ocean Technol 24:761–775
Nyeki S, Kalberer M, Colbeck I, de Wekker S, Furger M, Gäggeler H, Kossmann M, Lugauer M, Steyn D, Weingartner E, Wirth M, Baltensperger U (2000) Convective boundary layer evolution to 4 km a.s.l. over high-alpine terrain: airborne lidar observations in the Alps. Geophys Res Lett 27:689
Nyeki S, Eleftheriadis K, Baltensperger U, Colbeck I, Fiebig M, Fix A, Kiemle C, Lazaridis M, Petzold A (2002) Airborne lidar and in situ aerosol observations of an elevated layer, Leeward of the European Alps and Apennines. Geophys Res Lett 29:4
Pino D (2011) Boundary layer late afternoon and sunset turbulence. In: Presentation at special working group meeting of Eg-climet COST action, Palaiseau, April 2011
Ruffieux D, Stübi R (2001) Wind profiler as a tool to check the ability of two NWP models to forecast wind above highly complex topography. Meteorol Z 10:489–495
Stull R (1988) An introduction to boundary layer meteorology. Kluwer Academic Publishers, Dordrecht, 666 pp
Szintai B, Kaufmann P (2007) TKE as a measure of turbulence. In: Schättler U, Montani A, Milelli M (eds) Consortium for small-scale modelling. Newsletter, pp 2–9
Teschke G, Poenitz K (2010) On the retrieval of aerosol (mixing) layer heights on the basis of ceilometer data. In: International symposium for the advancement of boundary layer remote sensing, Paris, 28–30 June 2010, 4 pp
Vaisala (2007) Software manual lap-XM. Rev. 2.4.1.0. In: Technical references, 225 pp
Wang Z, Cao X, Zhang L, Notholt J, Zhou B, Liu R, Zhang B (2012) Lidar measurement of planetary boundary layer height and comparison with microwave profiling radiometer observation. Atmos Meas Tech 5:1965–1972
Weigel A (2005) On the atmospheric boundary layer over highly complex topography. Dissertation, ETH Zürich, 155 pp
Weingartner E, Nyeki S, Baltensperger U (1999) Seasonal and diurnal variation of aerosol size distributions ($10 < D < 750$nm) at a high-alpine site (Jungfraujoch 3580 m a.s.l.). J Geophys Res 104:26809–26820
Whiteman C (2000) Mountain meteorology: fundamentals and applications. Oxford University Press, New York, 355 pp

York D, Evensen N, Martnez M, de Basabe Delgado J (2004) Unified equations for the slope, intercept, and standard errors of the best straight line. Am J Phys 72:367

Zieger P, Kienast-Sjögren E, Starace M, von Bismarck J, Bukowiecki N, Baltensperger U, Wienhold F, Peter T, Ruhtz T, Collaud Coen M, Vuilleumier L, Maier O, Emili E, Popp C, Weingartner E (2012) Spatial variation of aerosol optical properties around the high-alpine site Jungfraujoch (3580 m a.s.l.). Atmos Chem Phys 12:7231–7249